Vision-and map-based non-line-of-sight satellites hybridized processing

David Bétaille, Cyril Meurie, Yann Cocheril

Vision- and map-based non-line-of-sight satellites hybridized processing

David Bétaille[1], Cyril Meurie[2] and Yann Cocheril[2]

Abstract— **Intelligent transportation systems use GNSS receivers as basic technological components. In urban applications one faces the problem of GNSS multipath and particularly of non-line-of-sight (NLOS) satellites. The development of GNSS receiver technologies for mass market encompasses the capability NLOS satellites processing by innovative techniques, not only based on the Signal to Noise Ratio, but also on vision or city model. This is particularly needed for urban positioning of cars for applications which require high accuracy and integrity, typically driving automation.**
This article deals with the detection of NLOS satellites among those tracked by an automotive-range receiver. We aim at developing a method jointly based on the analysis of video stream and a 3D map model of the environment. The article provides a literature review, an evaluation of some existing techniques and a preliminary analysis of the implementation of the retained algorithm on a prototype developed in the frame of a European H2020 "Fundamental Elements call" project.

I. INTRODUCTION

Global Navigation Satellites Systems (GNSS) widely contribute to the localization and navigation systems in Intelligent Transport Systems (ITS). However, as GNSS positioning relies on the propagation time measurement of at least 4 satellites simultaneously, their positioning performances are degraded in constraint environments such as urban zones. The impact of the surroundings of the antenna can be, first, unavailability of the service when signals are blocked, but also accuracy decrease in presence of multipath reception. Moreover, the case of Non-Line-Of-Sight (NLOS) signals - i.e. signals received after reflections on the surrounding obstacles with no direct ray - frequently occur in densely built environments and degrade localization accuracy because of the delay observed on the propagation time measurement when a reflection occurs. This delay creates an additional error on the pseudo-range measurement. In order to mitigate multipath impacts onto signal reception and tracking, a number of hardware solutions have been developed for a while by GNSS manufacturers, both at the antenna level and at the receiver level. This is not specifically the purpose of this research. In the meanwhile, many works focus on the development of solutions based on the complementarity of other sensors such as vision. Some of these solutions provide good results but are not yet integrated into embedded systems to be industrialized. This is one of the objectives of the eMAPs project. Another is to take advantage in this LOS/NLOS discrimination problem of local city map models, when available.

The development of GNSS receiver technologies for mass market encompasses the capability of NLOS satellites processing by innovative techniques, not only based on the Signal to Noise Ratio (SNR), but also on vision or city model. This is particularly needed for urban positioning of cars for applications which require high accuracy and high integrity, typically driving automation.

We aim at developing a method jointly based on the analysis of video streams and a 3D map model of the environment, in order to guarantee the detection of NLOS satellites among those tracked by an automotive-range receiver. This article is divided into four main parts. Section 2 gives a literature review. Section 3 is related to the NLOS detection based on vision. The definition of the retained algorithm for the sky/not-sky classification step is described and the validation is carried out on the experimental multi-sensors dataset created in Toulouse. Section 4 is related to the NLOS detection based on map model, including the description of the retained strategy that is applied in comparison to the vision-based strategy. Section 5 describes in deep the navigation results. Then we conclude on the work realized.

II. LITERATURE REVIEW

Literature focusing on techniques for localization performance enhancement in harsh environments is abundant. The most spread rely on multi-sensor-based approaches, for which the goals are to compensate the lack of performance of GNSS by adding other sensors (odometer, Inertial Measurement Unit, etc.). The number of sensors can increase the system complexity. Considering that, even with augmentation systems, multipath remain the main source of errors in localization systems, some studies investigate how to enhance accuracy by mitigating this specific source of errors [1]. Such techniques propose some exclusion procedures to avoid using corrupted data [2]. They can rely on GNSS observables such as SNR or the elevation angle [3] that can inform on pseudo-range reliability. Another approach consists in exploring the knowledge of the structure of the environment crossed by the vehicle for enhancing accuracy using vision. This part is specifically detailed below.

A. Review about NLOS detection using vision

This knowledge of the structure of the environment crossed by the vehicle can be extracted from video records or 3D models when available [4] [5] [6] [7] [8] [9].

[1]David Bétaille is with Structure et Instrumentation Intégrée, Univ Gustave Eiffel, COSYS-SII, F-44344 Bouguenais, France david.betaille@univ-eiffel.fr

[2]Cyril Meurie and Yann Cocheril are with Laboratoire Électronique Ondes et Signaux pour les Transports Univ Gustave Eiffel, COSYS-LEOST, F-59650 Villeneuve d'Ascq, France cyril.meurie@univ-eiffel.fr

Concerning, the first option, that is called direct, no a priori database or mapping is required. The structure can be obtained by images provided by several cameras installed on the roof of the vehicle. The approach has already been validated with the PREDISSAT tool [4] and is continuously improved in several research project (CAPLOC, SATLOC, ERSAT-GCC, SMARTIES, LOCSP and FERROMOBILE). In a first step, the state of reception of satellite signals is determined by comparing satellite positions and obstacle positions around the antenna. Satellites positioned in the sky area are directly visible: those behind the mask are NLOS. The information extracted from the image can allow us, for example, to exclude or weight, the satellites that degrade the receiver performances. In this way, the literature proposes different methods based on sky/not-sky classification using image processing. But most of them do not respect the real time constrain for embedded application or do not provide satisfactory results in complex urban environment. Some of which are proposed, tested and improved in the framework of research projects, but are not yet industrialized. This is why the eMAPs project aims to use the potential of the most promising methods by going to the end of the process, i.e. the industrialization of the complete embedded system. In the following, we present the different categories of NLOS detection methods based on image processing, called direct, and detail, for each of them, the most relevant papers of the state-of-the-art regarding the eMAPs project.

As introduced previously, during the last decade, we have seen a strong growth of research works using computer vision for applications related to localization systems. They can be classified into different categories. First of all, we can distinguish methods using perspective images and other solutions based on omnidirectional images allowing a wider field of view. In the framework of the eMAPs project and the eHermes prototype, we focus on the second approach. Secondly, one can classify the proposed approaches into different categories. The first one consists in using methods based on matching algorithms to find, from a database of georeferenced images, the image closest to the requested image [10] [11] [12]. The second one consists in using images (mainly omnidirectional) coupled with 3D models to detect the skyline separating the sky from other objects in the environment (vegetation, bridge, building, etc.) [13] [5] [14]. The third one consists in using omnidirectional image to detect the skyline and classify the pixels/regions of the acquired image as sky (respectively non-sky) in order to identify, after repositioning in the image, satellite classified LOS (respectively NLOS). This is the last category that we retain for the real-time detection task of the LOS/NLOS satellites of the eMAPs project. The methods of this category, which are likely to be appropriate, can also be classified with a finer level of detail, depending on whether they deal with:

- image segmentation or unsupervised clustering [16] [15] [18] [17] [19] [20] [21] [22] [23];
- machine learning, big-data or deep-learning [17] [24] [21] [25] [26] [27] [28];
- specific sensors such as infrared cameras [29] [5];
- dedicated on FPGA architecture [30] [31].

To summarize the literature review on LOS/NLOS vision-based and conclude, current state-of-the-art approaches use convolutional neural networks to segment image into sky vs non-sky regions. They offer in certain case better results compared to more classical strategies but require a powerful training process, dedicated hardware and a huge computational time when large scenario coverage is aimed. This is for this reason, that we will not retain these types of approach in the framework of eMAPs project. Other works, most of which are older, but which offer very interesting performances focus on so-called more classical clustering techniques. They are applied on infrared, multispectral, or visible images. We can now reject the methods developed for infrared images because of the type of cameras embedded in the eHermes prototype. The other methods used in the visible domain are mainly methods based on: edge detection (Sobel, Canny), automatic and non-parametric image thresholding (Otsu), supervised (SVM, k-NN, Bayes, Neural Networks...) or unsupervised clustering (Fisher, K-means, Fuzzy C-means...). They can also combine more in-depth methods used in pre-processing of the clustering step such as color space changes or segmentation methods based on graph analysis, on superpixels or combining various complementary characteristics such as texture, luminosity, points of interest, etc. The comparison of the performance of the vision-based algorithms proposed in the framework of sky/non-sky detection for the improvement of the localization is often discussed in research papers. It allows us to carry out cross-checks to isolate the most interesting approaches. In our opinion, edge detection methods are not adapted to the high complexity of the urban environment in which the eHermes system will be used. Classification approaches that are coupled with a pre-processing step based for example on superpixels segmentation or combining complementary features are to be avoided due to the low speed/performance gain. Unsupervised or supervised classification techniques seem to be the most suitable and preferred approaches. Several studies have shown that the Fisher algorithm used on a simplified image offers very good results on real dataset acquired with a fisheye camera as well as SVM but with a higher processing time. This one seems to us relevant as well as the Otsu algorithm which has been recognized for several years and by several authors as very interesting in terms of performance and processing time. Considering the real-time detection task of the LOS/NLOS satellites in the eMAPs project, we will therefore focus on these two approaches by giving the advantage to the Otsu algorithm for its computational cost and its easy integration on a FPGA board.

B. Review about NLOS detection using map model

As indicated in introduction, an alternative exists to detect NLOS satellites, which is indirect, making use of a digital map into which an a priori user location is projected. The use of geometric city models in urban canyons has first

been addressed simultaneously by [32] and [33]. Next, a few research teams have been active: [34] [35] [36], coupling 3D modelling with road plane or numerical terrain 2D constraints. Sky plot of building boundaries from the perspective of the user is made popular at that time.

Whereas these articles present methods that do not model the additional path delay due to signal reflection, a few others, on the contrary, will actually make this next step forward: [37] [38] [8] [9] [39]. In addition to this LOS/NLOS indirect methodology, shadow matching leverages the possibility of predicting which satellites will be visible from the point of view of the user, and compares this prediction to the actual observation [40] [41] [42]. One can restrict the user's location domain by considering those satellites present in the ephemeris and for which no measurement is made. Whilst [8] introduced urban trench modelling of the street (UTM: Urban Trench Model), more recent development [43] got rid of this geometrical approximation, to take advantage of the full polygonal description of the buildings, instead of considering simple parallelepiped streets. This methodology (UMM: Urban Multipath Model) is presented in section 3. Despite several proofs of concept for map aided GNSS location through LOS/NLOS detection, there is still need for large scale experiment and results, unless the methodology cannot be generalized. This is one of the purposes of this research in eMAPs, the other being the comparison with vision-based.

III. NLOS DETECTION BASED ON VISION

Considering our analysis of the state-of-the-art, it seems judicious to use the Otsu algorithm in the sky/non-sky classification task in the framework of the eMAPs project. Indeed, this method is relatively simple to implement, does not require any specific hardware, and has a reduced calculation time. These are all reasons why it is often used in the vision aided GNSS applications. Thus, we recall, the principle and the definition of the algorithm given in details in [44] and synthetized in [19].

Algorithm 1 Summary of Otsu algorithm

1. Compute the histogram (the number of occurrences for each intensity level) and the probability of each intensity level p_i
2. Set the initial values $P_0(0)$ and $P_1(0)$ and their initial corresponding means $\mu_{I_{C0}}(0)$ and $\mu_{I_{C1}}(0)$
3. Set through all possible thresholds from 1 to L :
3.1. Update P_0, P_1 and $\mu_{I_{C0}}$ and $\mu_{I_{C1}}$
3.2. Compute the inter-class variance α_k^2
4. The desired threshold k^* corresponds to the maximum of α_k^2

Otsu algorithm is a non-parametric and unsupervised method based on an automatic threshold selection currently used in image segmentation. It allows to binarize an image by analysing its histogram and calculating an optimal threshold. This threshold value used to classify the pixels of the image into one of the two possible classes (sky and non-sky in our works) is the one that maximizes the interclass variance.

The eMAPs dataset (see section V) contains 43683 images acquired in the area of Toulouse with the fisheye camera oriented toward the sky for the NLOS detection task. The sky/not-sky classification procedure based on Otsu algorithm has been tested on the entire dataset and provide visual satisfactory results. Nevertheless, to provide quantitative results, we have calculated four classical metrics used actually in artificial intelligence domain: accuracy, recall, precision and f1-score. These metrics require a ground truth of the sky/not-sky classification but which cannot be carried on the whole dataset because of the time involved, a problematic well know of the research community. To solve this problem, we have created a reduced dataset (with a frame rate of 250) containing 175 images evenly distributed along the course. The corresponding reference classification has been handmade created by four experts with the Computer Vision Annotation Tool. Figure 1 illustrates four fisheye images acquired in different environments during the experimentation (line 1), the output classification provided by Otsu algorithm (line 2), the corresponding temporary ground truth image created with CVAT (line 3). the LOS/NLOS satellites detection after repositioning in the current image (line 4). In this line, LOS (respectively NLOS) satellites are marked in green color (respectively in red color).

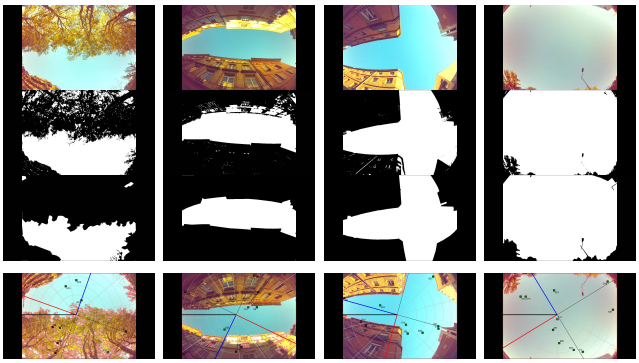

(a) #8500 (b) #17750 (c) #19000 (d) #31250

Fig. 1. LOS/NLOS satellites detection by vision

Thus, on this reduced dataset, the sky/not-sky classification results based on Otsu algorithm obtains an accuracy of 93.16 %, a recall of 99.96%, a precision of 89.95% and a f1-score of 93.66%. Figure 2 illustrates the different metrics calculated on each image of the reduced dataset. It permits to shows if the classification results are constant or if some images are more difficult to treat. Globally, the f1-score is upper to 80% whatever the image considered expect for 3 slots regrouping 9 images over 175 images. Indeed, as we can notice in Figure 2, three slots show a decrease of the performance: the first one (images 21-23) shows a minimum at 44%, the second one (images 86-88) is lower at 32% and the last one (images 93-96) is the worse at 16%. These classification errors are all due vegetation in the images.

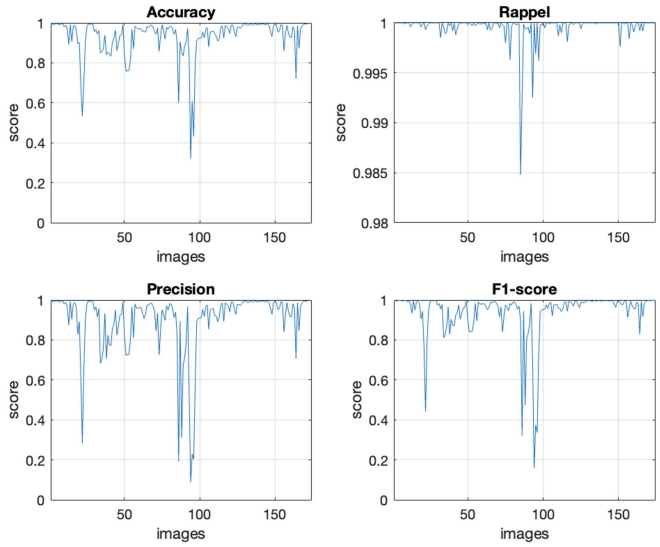

Fig. 2. Sky/not-sky classification results on the reduced eMAPs dataset, compared to the ground truth and using the classical metrics: accuracy, recall, precision and f1-score

IV. NLOS DETECTION BASED ON MAP MODEL

The basic idea is to project the current rover position estimate into a 3D map model and determine, from this point of view, whether or not satellites are LOS or NLOS. The rover position estimate could be:

- either the one based on the GNSS only observations
- or the one based on GNSS hybridized with other sensors, e.g. wheel speed, IMU, visual odometry...

In test, the ground truth can also be used instead of the rover position, to estimate best feasibility.
The 3D map model, in the context of this research, makes use of the French national database, BD Topo ®. This is available everywhere in France, with approximately 3 years age. The building layer is used, i.e. polygons representing buildings and their average height. In order to keep reasonable computational throughput, a selection in the map data should be made. This has been specified in accordance with the itinerary performed for test purpose in section V.

The LOS/NLOS decision based on 3D map model is returned to the GNSS navigation algorithm in order to e.g. reweight the GNSS observations depending on the LOS/NLOS decision. In addition to this decision, the methodology is capable of computing a ranging correction in NLOS case. This correction can be applied by the navigation algorithm. The process is first to detect if any facade exists in every satellite azimuth, with a height enough to occult the corresponding satellite elevation. This initial step identifies LOS/NLOS satellites. The next step is to examine every facade, locally, to detect whether it could make a specular reflection with the occulted satellite previously identified. In this case, the final step is to check that no other facade may occult the reflected ray, whether in between the antenna and the impact point, or whether in between the impact point and the satellite. In case several facades exist with reflected rays, the one with the largest incidence angle is preferred. Facades are regarded as vertical planes, with the height of the polygon they belong to. There are several options finally, but the one suggested by Ni Zhu in her PhD dissertation [43] relies on both functional and stochastic approaches. For those satellites being NLOS: ranging are corrected, using the additional travelled paths estimated with the 3D map model (functional) and ranging are reweighted in the least-squares of Kalman filter GNSS navigation algorithm: their variances are multipied by 10 (stochastic).

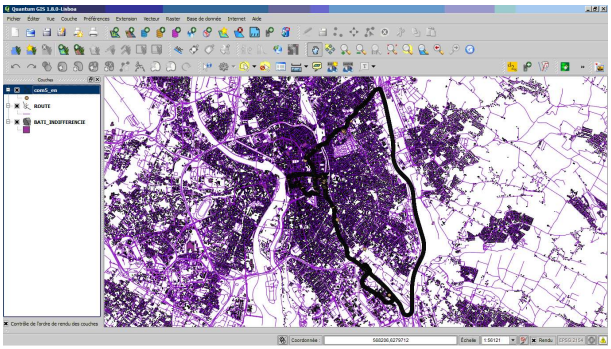

Fig. 3. One hour loop in Toulouse

V. NAVIGATION RESULTS

A. Experimental setup

An acquisition campaign has been carried out in the city of Toulouse, on 23 April 2021 (Figure 3). There are two sections, initial and final, in urban environment, and an intermediate section, on the south ad east highways of Toulouse. The total duration of the test is 62 minutes: 56 minutes in the city centre and 6 minutes on the highway. 5 minutes (between 17:14 and 17:19) in the very deep centre of the city have been chosen to focus on in the analysis. In addition to the skyward facing camera, the GNSS equipment on-board the vehicle was, in addition to a Ublox F9P multi-constellation receiver, a Novatel SPAN GNSS inertial navigation system, for ground truth purpose, continuously available and reliable (i.e. dm accurate).

B. Global confusion matrix

A confusion matrix has been computed in order to compare both methodologies of LOS/NLOS classification using vision and map. The rover position used for map-based LOS/NLOS decision was, for feasibility purpose, the reference trajectory or ground truth. We prove, in the deep centre of Toulouse, that LOS/NLOS classification disagreement between both methods will not occur for more than 12% of the total number of satellite observations.

In the deep urban centre, one counts 1501 epochs with GPS measurements (5 minutes @ 5 Hz) on 23 April 2021 in Toulouse. This totalizes 11821 measurements, among which the elevation and azimuth of 7270 satellites have their projection in the fisheye field.

The LOS/NLOS confusion matrix for fisheye vision versus map model classifications is given in Table I.

TABLE I

CONFUSION MATRIX OBTAINED BY VISION VERSUS MAP MODEL

	LOS by vision	NLOS by vision
LOS by map model	5953 images: 81.9%	401 images: 5.5%
NLOS by map model	502 images: 6.9%	414 images: 5.7%

C. Navigation results based on 3D model

The navigation solvers used are a GPS-only ordinary least-squares (OLS), in which every satellite has the same weight, and a weighted least-squares (WLS), similar as RTKLIB with usual modelling of range errors, in which the variance equals:

$$\sigma^2_{GPS} = 0.3^2 + 0.3^2/sin(el) + 2.4^2 + 0.3^2 + 0.3^2 + 0.5^2 \quad (1)$$

where 2.4m stands for orbit error, 0.3m for receiver noise, 0.3m and 0.5m for iono and tropospheric errors resp. Broadcasted ephemeris are used (tlse113z.21n). An elevation cutoff of 15° is optional.

In case of NLOS satellite, a geometrical correction is applied, and the satellite is downweighted by a factor 10 (i.e. variance*10). LOS/NLOS decision and range correction are based on the ground truth in this computation.

The plane error (HPE: horizontal positioning error) is computed and given in Table II, i.e. the quadratic sum of East and North (E, N) deviations between the GPS solutions and the reference trajectory.

TABLE II

NAVIGATION RESULTS: PLANE ERROR (HPE)

Each cell displays median, 68 and 95 percentiles of HPE	Highway 1855 ep	City centre 16791 ep	City centre 16791 ep map-aided
OLS no el mask (no ep w/o solution)	1.23m 1.47m 2.21m	2.71m 5.90m 32.33m	/
WLS no el mask	1.21m 1.47m 2.21m	2.69m 5.83m 30.90m	2.33m 4.87m 26.54m
OLS el>15° (13 ep w/o solution)	1.80m 2.08m 2.95m	2.43m 3.03m 24.26m	/
WLS el>15°	1.79m 2.08m 2.95m	2.43m 3.03m 24.19m	2.40m 3.00m 19.44m

The plane error envelop (HPL: horizontal protection level), i.e. the semimajor axis of the plane error ellipse, is computed and given in Table III, with a probability of missed detection PMD of 0.1% and dimension 4 (for E, N, Up and receiver clock term), which is supposed to bound 99.9% of the plane error. Note that, before computing this HPL, a global test is made, in order to select only reliable solutions. This test, a $\chi 2$ test based on the sum of weighted residuals, eliminates solutions with a probability of false alarm PFA of 0.1%. The degree of freedom applicable in this test equals the number of used satellites minus 4.

In this table, we focus on results in the city only, and for weighted least-squares. The misleading information (MI) is also indicated, i.e. the rate of HPE being actually over HPL, violating the computed integrity.

TABLE III

NAVIGATION RESULTS: PROTECTION LEVEL (HPL)

Each cell displays median, 68 and 95 percentiles of HPL	City centre 16791 epochs	City centre 16791 epochs map-aided
WLS no el mask	71.5% global test ok	78.9% global test ok
	7.33m 8.64m 18.14m 18.1% violation	7.65m 11.00m 31.99m 1.6% violation
WLS el>15°	88.1% global test ok	92.2% global test ok
	11.68m 12.18m 21.87m 7.8% violation	11.96m 12.95m 43.60m 1.8% violation

A particular focus, Table IV, is made onto the 5 minutes subset in the deep city centre of Toulouse.

TABLE IV

NAVIGATION RESULTS IN THE DEEP CITY CENTRE: HPE AND HPL

Each cell displays median, 68 and 95 percentiles	Deep city centre 1501 epochs	Deep city centre 1501 epochs map-aided
WLS no el mask	9.78m 16.95m 31.51m	8.85m 11.20m 20.22m
	27.2% global test ok	76.7% global test ok
	14.03m 15.24m 25.46m 25.7% violation	25.56m 26.77m 36.75m 1.6% violation
WLS el>15°	8.36m 10.70m 22.75m	4.65m 7.68m 14.74m
	74.5% global test ok	96.7% global test ok
	17.70m 17.90m 21.68m 14.4% violation	25.57m 28.07m 48.14m 1.2% violation

The improvement for GPS-only with no elevation cutoff is around 0.3m less on the median plane error in Toulouse urban test globally (after removing the highway). One gets 2.33m instead of 2.69m, applying the NLOS downweighting and correction. This is in the city centre. The 68 and 95 percentiles are improved by resp. 1 and 4 meters. Almost the same accuracy seems achievable with a 15° cutoff, which would disqualify the map-based NLOS correction, even based on ground truth. However, removing satellites below 15° elevation increases error on the highway, by 0.6m approx. Hence, keeping all satellites, even low in elevation, with NLOS detection and correction seems rather valuable. Moreover, the combination of this 15° cutoff with NLOS detection and correction gives the best results, with a median plane error still equal to 2.40m but with improved 68 and 95 percentiles. An examination into details of samples of the trajectory in the deep urban centre of Toulouse have also be carried out. This shows that UMM does bring improvement

when combined again the elevation cutoff. In the case of 15° elevation mask and UMM, the best accuracy is obtained. This indicates that UMM calculation is applicable and valuable to satellites above this elevation mask.

At first analysis, results are positive in Toulouse, even if not so impressive compared to what we used to obtain in Nantes and, above all, in Paris. Note that formerly, we also experienced slightly less success in applying UMM in Toulouse, except in the urban city centre. Globally, Toulouse streets are very different from Paris Haussmannian streets. (UTM was not that good approximating in Toulouse.) Another challenge is to measure the improvement by UMM on the same version of the navigation algorithm, i.e. every other tuning (in particular stochastic parameters) being unchanged. This was not the case in several of our previous works neither in some other articles one can read about map-aided navigation. It is non sense e.g. comparing an OLS with a map-based WLS. Both should be weighted or not, with modulations due to the use of the 3D city model.

For further works, we aim at investigating again with the same algorithms our former data sets, in 2012, 2014 and 2019, in Nantes, Paris and Toulouse. Some are running the F9P (the latter), some the LEA 6T from Ublox. Again, the impact of the ionosphere should be regarded carefully, in particularly in 2014 where it was maximum and not properly modelled in our previous investigations [45]. Note that range downweighting in NLOS case mechanically increases protection level, leading to less integrity failure. An alternative, in order to keep almost constant envelop, would be to upweight all other ranges in LOS case.

D. Navigation results based on vision

Instead of map-based, one suggests in this last part to move to vision-based (for those satellites projecting in the fisheye field of view). In this case, no range correction is made, but only downweighting in NLOS case. In short (Table V), the introduction of vision-based LOS/NLOS sorting in the solver does not change much to the results already shown. They remain almost unchanged. In the deep centre of Toulouse, we have 4.65m of median error against 7.03m for fisheye sorting (8.36m if we do nothing).

TABLE V
VISION-AIDED NAVIGATION RESULTS: PLANE ERROR (HPE)

Each cell displays median, 68 and 95 percentiles of HPE	City centre 16791 epochs vision-aided	Deep city centre 1501 epochs vision-aided
WLS no el mask	2.69m 5.95m 32.18m	8.53m 17.02m 32.22m
WLS el>15°	2.41m 3.00m 25.76m	7.02m 10.72m 24.42m

Since we know that both sorts match 88% in Toulouse, one can assume that the ranging correction makes a significant difference in the very final navigation results, because downweighting only seems not so efficient.

VI. CONCLUSION

This article is based on the research and development activities on the vision subsystem of the GNSS eHermes platform, delivered during the eMAPs H2020 project. The vision-based GNSS is challenged with a 3D model-based LOS/NLOS satellite processing.

The first part of the article summarises an analysis of the current state-of-the-art of the NLOS detection based either on vision or on 3D map. At this stage, Otsu algorithm seems to be promising for the vision-based NLOS detection on the eHermes prototype. The second part is devoted to the description of the NLOS detection based on vision and the evaluation of the performance of the retained Otsu algorithm. The evaluation concludes that Otsu algorithm yields good results: a good classification rate around 96% and a computational time of 27ms/frame on the experimental multi-sensors dataset created by ENAC during the eMAPs project in Toulouse. The third part is devoted to the NLOS detection based on 3D map model using the French national database, BD Topo ®. The methodology based on the detection of satellite occluding facade and the possible reflecting ones is described. The jointly use of functional and stochastic approaches combined seems to be an interesting and promising way. Finally, a comparison between vision-based and map-based LOS/NLOS processes has been carried on a focus of 5 minutes in the very deep centre of the Toulouse city. Both techniques agree by 88% with an advantage, in terms of accuracy, using the map and the inferred additional pseudo-ranges, if NLOS, due to building reflections.

Additional work is on-going in order to finalize the eHermes implementation and also to generalize the processes to other satellites than GPS only. Trying to keep reasonable protection level, not increased PL due to downweight of NLOS ranges, is also targeted in further research about aided urban navigation.

ACKNOWLEDGEMENT

These research investigations have been carried out in the frame of the eMAPs European H2020 "Fundamental Elements call" project. The authors warmly thank the project leader Benjamin Kawak, 3DAerospace, as well as Paul Thévenon, ENAC and his post-doc Jan Bolting, for developing the eHermes prototype and providing the experimental framework and data in Toulouse.

REFERENCES

[1] Lentmaier, M., Krach, B., Robertson, P. (2008), Bayesian Time Delay Estimation of GNSS Signals in Dynamic Multipath Environments, Hindawi Publishing Corporation, International Journal of Navigation and Observation, Vol. 2008, Article ID 372651, 11p.

[2] Pervan, B.S., Lawrence, D.G., Cohen, C.E., Parkinson, B.W. (1996), Parity space methods for autonomous fault detection and exclusion using GPS carrier phase, Position Location and Navigation Symp., pp. 649–656.

[3] Wang, J.-H., Gao, Y. (2007), High-Sensitivity GPS Data Classification Based on Signal Degradation Conditions, IEEE Tr. on Vehicular Technology, Volume 56, Issue 2, pp. 566–574.

[4] Marais, J., Berbineau, M., Heddebaut, M. (2005), Land Mobile GNSS, Availability and Multipath Evaluation Tool, IEEE Tr. On Vehicular Technology, Vol. 54, Issue 5, pp. 1697-1704.

[5] Meguro, J. -I., Murata, T., Takiguchi, J. -I., Amano, Y., and Hashizume, T. (2009). GPS Multipath Mitigation for Urban Area Using Omnidirectional Infrared Camera. IEEE Tr. on Intelligent Transportation Systems, 10(1), 22-30.

[6] Meurie, C., Ruichek, Y., Cohen, A., Marais, J. (2010), An hybrid an adaptive segmentation method using color and textural information, IS&TSPIE Electronic Imaging 2010 - Image Processing: Machine Vision Applications III, Proc. of SPIE-IS&T Electronic Imaging, SPIE Vol. 7538, 11p., California USA.

[7] Marais, J., Meurie, J., Attia, D., Ruichek, Y., Flancquart, A (2013). Toward accurate localization in guided transport: combining GNSS data and imaging information. Transportation research. Part C, Emerging technologies, Elsevier, 15p.

[8] Bétaille, D., Peyret, F., Ortiz, M., Miquel, S. and Fontenay, L. (2013a). A New Modelling based on Urban Trenches to Improve GNSS Positioning Quality of Service in Cities. IEEE Intelligent Transportation Systems Mag., Vol. 5, No. 3, 59–70.

[9] Bétaille, D., Peyret, F., Ortiz, M., Miquel, S. and Fontenay, L. (2013b). GNSS Accurate Positioning Including Satellite Visibility Check in a Multiple Hypotheses 3D Mapping Framework. ENC GNSS Congress, Vienna.

[10] Zhang, W. and Kosecka, J. (2006). Image based localization in urban environments. 3D Data Processing Visualization and Transmission.

[11] Jacobs, N., Satkin, S., Roman, N., Speyer, R., and Pless, R. (2007). Geolocating static cameras. International Conf. on Computer Vision.

[12] Hays, J. and Efros, A. (2008). Im2gps: estimating geographic images from single images. Computer Vision and Pattern Recognition.

[13] Koch, O., and Teller, S. (2007). Wide-Area Egomotion Estimation from Known 3D Structure. IEEE Conf. on Computer Vision and Pattern Recognition, 1-8.

[14] Ramalingam, S., Bouaziz, S., Sturm, P., and Brand, M. (2010). SKYLINE2GPS: Localization in urban canyons using omni-skylines. IEEERSJ International Conf. on Intelligent Robots and Systems, 3816-3823.

[15] Cohen, A., Meurie, C., Ruichek, Y., and Marais, J. (2010). Characterization of the reception environment of GNSS signals using a texture and color based adaptive segmentation technique. IEEE Intelligent Vehicles Symp., 275-280.

[16] Cohen, A., Meurie, C., Ruichek, Y., Marais, J., and Flancquart, A. (2009). Quantification of GNSS signals accuracy: An image segmentation method for estimating the percentage of sky. IEEE International Conf. on Vehicular Electronics and Safety, 35-40.

[17] Attia, D., Meurie, C., Ruichek, Y., and Marais, J. (2011). Counting of satellites with direct GNSS signals using Fisheye camera: A comparison of clustering algorithms. 2011 14th International IEEE Conf. on Intelligent Transportation Systems (ITSC), 7-12.

[18] Attia, D., Meurie, C., Ruichek, Y., Marais, J., and Flancquart, A. (2010). Image analysis based real time detection of satellites reception state. 13th International IEEE Conf. on Intelligent Transportation Systems, 1651-1656.

[19] Gakne, P. V., and Petovello, M. (2015). Assessing image segmentation algorithms for sky identification in GNSS. International Conf. on Indoor Positioning and Indoor Navigation (IPIN), 1-7.

[20] Suzuki, T., and Kubo, N. (2014). N-LOS GNSS signal detection using fish-eye camera for vehicle navigation in urban environments. 27th International Technical Meeting of the Satellite Division of the Institute of Navigation, 3, 1897-1906.

[21] Middel, A., Lukasczyk, J., Maciejewski, R., Demuzere, M., and Roth, M. (2018). Sky View Factor footprints for urban climate modeling. Urban Climate, 25, 120-134.

[22] Laungrungthip, N., McKinnon, A. E., Churcher, C. D., and Unsworth, K. (2008). Edge-based detection of sky regions in images for solar exposure prediction. 23rd International Conf. Image and Vision Computing New Zealand, 1-6.

[23] Pavlovic, A., Gavrovska, A., and Milosavljevic, N. (2018). The Skyline Image Segmentation using Color and Detail Clustering. 14th Symp. on Neural Networks and Applications (NEUREL), 1-5.

[24] Nice, K. A., Wijnands, J. S., Middel, A., Wang, J., Qiu, Y., Zhao, N., Thompson, J., Aschwanden, G. D. P. A., Zhao, H., and Stevenson, M. (2020). Sky pixel detection in outdoor imagery using an adaptive algorithm and machine learning. Urban Climate, 31, 100572.

[25] Song, Y., Luo, H., Ma, J., Hui, B., and Chang, Z. (2018). Sky Detection in Hazy Image. Sensors, 18(4), 1060.

[26] Place, C. L., Urooj, A., and Borji, A. (2019). Segmenting Sky Pixels in Images: Analysis and Comparison. IEEE Winter Conf. on Applications of Computer Vision (WACV), 1734-1742.

[27] Badrinarayanan, V., Kendall, A., and Cipolla, R. (2017). SegNet: A Deep Convolutional Encoder-Decoder Architecture for Image Segmentation. IEEE Tr. on Pattern Analysis and Machine Intelligence, 39(12), 2481-2495.

[28] Boker, C., Niemeijer, J., Wojke, N., Meurie, C., and Cocheril, Y. (2019). A System for Image-Based Non-Line-Of-Sight Detection Using Convolutional Neural Networks. IEEE Intelligent Transportation Systems Conf., 535-540.

[29] Meguro, J. -I., Murata, T., Takiguchi, J. -I., Amano, Y., and Hashizume, T. (2008). GPS accuracy improvement by satellite selection using omnidirectional infrared camera. IEEE/RSJ International Conf. on Intelligent Robots and Systems, 1804-1810.

[30] Wang Jianlai, Yang Chunling, Zhu Min, and Wang Changhui. (2009). Implementation of Otsu's thresholding process based on FPGA. 4th IEEE Conf. on Industrial Electronics and Applications, 479-483.

[31] Pandey, J. G., Karmakar, A., Shekhar, C., and Gurunarayanan, S. (2014). A Novel Architecture for FPGA Implementation of Otsu's Global Automatic Image Thresholding Algorithm. 2014 27th International Conf. on VLSI Design and 13th International Conference on Embedded Systems, 300-305.

[32] Bradbury, J., Ziebart, M., Cross, P. A., Boulton, P. and Read, A. (2007). Code Multipath Modelling in the Urban Environment Using Large Virtual Reality City Models: Determining the Local Environment. The Journal of Navigation, 60, 95–105.

[33] Suh, Y. and Shibasaki, R. (2007). Evaluation of Satellite-Based Navigation Services in Complex Urban Environments Using a Three-Dimensional GIS. IEEE Tr. on Communications, Vol. E90-B, No. 7, 1816–1825.

[34] Wang, L., Groves, P. D. and Ziebart, M. (2012). Multi-Constellation GNSS Performance Evaluation for Urban Canyons Using Large Virtual Reality City Models. The Journal of Navigation, 65, 459–476.

[35] Obst, M., Bauer, S., Reisdorf, P. and Wanielik, G. (2012). Multipath Detection with 3D Digital Maps for Robust Multi-Constellation GNSS/INS Vehicle Localization in Urban Areas. Proceedings of the IEEE Intelligent Vehicles Symp., Alcalá de Henares.

[36] Peyraud, S., Bétaille, D., Renault, S., Ortiz, M., Mougel, F., Meizel, D. and Peyret, F. (2013) About Non-Line-Of-Sight Satellite Detection and Exclusion in a 3D Map-Aided Localization Algorithm. Sensors, 13, 829–847.

[37] Bourdeau, A., Sahmoudi, M. and Tourneret, J.-Y. (2012). Tight Integration of GNSS and a 3D City Model for Robust Positioning in Urban Canyons. Proceedings of the 20th International Technical Meeting of the Satellite Division of The Institute of Navigation, Nashville, TN.

[38] Miura, S., Hisaka, S. and Kamijo, S. (2013). GPS Multipath Detection and Rectification using 3D Maps. Proceedings of the IEEE Intelligent Transportation Systems Conf., The Hague.

[39] Suzuki, T. and Kubo, N. (2013). Correcting GNSS Multipath Errors Using a 3D Surface Model and Particle Filter. Proceedings of the 26th International Technical Meeting of The Satellite Division of the Institute of Navigation, Nashville, TN.

[40] Groves, P. D. (2011). Shadow Matching: A New GNSS Positioning Technique for Urban Canyons. The Journal of Navigation, 64, 417–430.

[41] Wang, L., Groves, P. D. and Ziebart, M. (2013). GNSS Shadow Matching: Improving Urban Positioning Accuracy using a 3D City Model with Optimized Visibility Scoring Scheme. Navigation, Vol. 60, 195–207.

[42] Yozevitch, R., Boaz B-M and Amit D. (2014). GNSS accuracy improvement using rapid shadow transitions. IEEE Transactions on Intelligent Transportation Systems 15, no. 3.

[43] Zhu, N. (2018). GNSS propagation channel modelling in constrained environments: Contribution to the improvement of the geolocation service quality. PhD dissertation Univ. de Lille / Ifsttar.

[44] Otsu, N. (1979). A Threshold Selection Method from Gray-Level Histograms. IEEE Tr. on Systems, Man, and Cybernetics, 9(1), 62-66.

[45] Rivoal, D., Bossard, Q., and Bétaille, D. (2021). A benchmark of the GPS+Galileo F9P receiver, 14th Annual Baska GNSS Conf., Krk island Croatia.